RSC Advances

PAPER

View Article Online
View Journal | View Issue

Cite this: *RSC Adv.*, 2022, **12**, 7712

Methyl nitrate energetic compounds based on bicyclic scaffolds of furazan–isofurazan (isoxazole): syntheses, crystal structures and detonation performances†

Qi Xue,[ab] Fuqiang Bi,[ab] Yifen Luo,[ab] Jiarong Zhang,[ab] Kaidi Yang,[ab] Bozhou Wang *[ab] and Ganglin Xue *[c]

Two energetic bicyclic scaffolds (furazan–isoxazole and furazan–1,3,4-oxadiazole) were constructed *via* different cyclization reactions. Based on the energetic bicyclic scaffolds, the energetic compounds, 3-(4-nitraminofurazan-3-ly)-isoxazole-5-methylnitrate **1c** and 5-(4-nitraminofurazan-3-ly)-1,3,4-oxadiazole-2-methylnitrate **2c**, were designed and synthesized in good yields. Because of the acidity of nitramine, the corresponding energetic ionic salts, ammonium 3-(4-nitraminofurazan-3-ly)isoxazole-5-methylnitrate **1d** and ammonium 5-(4-nitraminofurazan-3-ly)-1,3,4-oxadiazole-2-methylnitrate **2e**, were also obtained and well characterized, their structures were further determined by X-ray single crystal diffraction. To have a better understanding of the structure–property relationships of furazan-bicyclic scaffolds and nitrate groups, their thermal behaviors, detonation performances and the sensitivities were investigated *via* differential scanning calorimetry (DSC), ESP analysis, Hirshfeld surfaces calculation, EXPLO5 program and BAM standard techniques. Compared with those of ammonium 5-(4-nitraminofurazan-3-ly)-1,2,4-oxadiazole-2-methylnitrate **3e**, the results show that all these methyl nitrate energetic compounds based on bicyclic scaffolds of furazan–isofurazan exhibit good detonation performances and extraordinary insensitivities. As supported by experimental and theoretical data, the formation of energetic ionic salts causes an increase of the weak interactions, significantly improving the thermal performance over 110 °C.

Received 12th January 2022
Accepted 23rd February 2022

DOI: 10.1039/d2ra00215a

rsc.li/rsc-advances

Introduction

Since the discovery of the nitroglycerin (NG) by Ascanio Sobrero in 1874, nitrate ester compounds have been widespread and used in diversified fields, including medicines,[1–4] fuel additives,[5,6] and especially in military fields.[7–10] On the one hand, the nitrate ester group could be easily synthesized in high yield by treatment of the corresponding alcohols with concentrated nitric acid or a nitrating mixture.[11] On the other hand, introducing a nitrate ester group is an effective means to increase the energetic performance and oxygen balance of energetic molecules. Up to now, the aliphatic nitrate ester energetic compounds have been widely used as primary explosives, secondary explosives, and plasticizer ingredients for military purposes, such as nitroglycerin (NG),[12] pentaerythritol tetranitrate (PETN),[13] xylitol pentanitrate (XPN)[14] (Fig. 1(a)). However, accompanied by high performances and great compatibility, these compounds often present high mechanical sensitivities and low thermal decomposition temperature, which greatly influence their handling safety.

In recent years, there are a few examples of heterocyclic-based nitrate ester compounds have been reported.[15–19] In particular, the recently synthesized bis(1,2,4-oxadiazole) bis(methylene)dinitrate (BOM) displays calculated detonation pressure 50% higher than that of TNT and exhibits a relatively high decomposition temperature and lower sensitivities to impact and friction compared with RDX.[19] Compared with aliphatic nitrate ester compounds, the thermal stability of heterocyclic-based nitrate ester compounds is significantly improved due to π–π stacking effect of heterocyclic skeleton and some of them can be used as melt-castable explosives (Fig. 1(b)). For example, with the same number of nitrate ester groups, 3,3′-biisoxazole-4,4′,5,5′-tetra(methylene)tetranitrate (BITN)[16] and 4,5-bis(nitrooxy methylene)-1*H*-1,2,3-triazole-1-ethyl nitrate (PN3)[20] have higher melting points, density

[a]*Xi'an Modern Chemistry Research Institute, Xi'an, 710065, China. E-mail: wbz600@163.com*

[b]*State Key Laboratory of Fluorine & Nitrogen Chemicals, Xi'an, 710065, China*

[c]*College of Chemistry & Materials Science, Key Laboratory of Synthetic and Natural Functional Molecule Chemistry, Northwest University, Xi'an 710127, China. E-mail: xglin707@163.com*

† Electronic supplementary information (ESI) available. CCDC 2131217 and 2131218. For ESI and crystallographic data in CIF or other electronic format see DOI: 10.1039/d2ra00215a

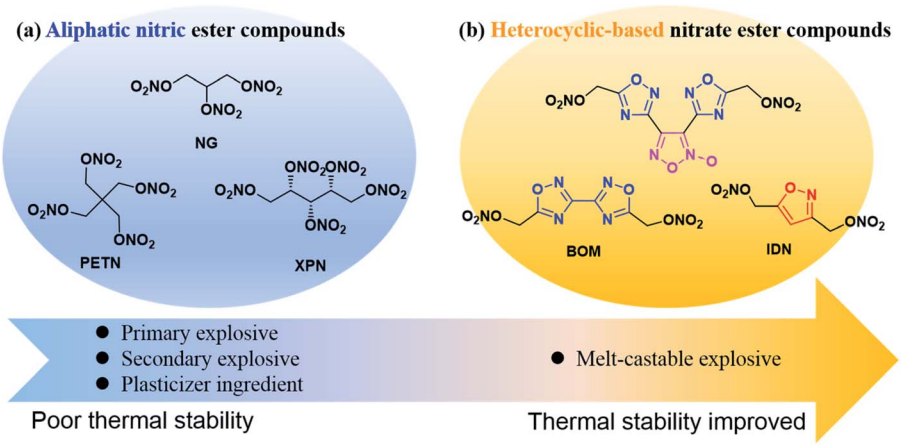

Fig. 1 Representative examples: (a) typical aliphatic nitrate ester energetic compounds. (b) Typical heterocyclic-based nitrate ester compounds.

thermal decomposition temperatures than those of PETN and NG (Scheme 1(a) and (b)), respectively. However, the mechanical sensitivity performance of heterocyclic-based nitrate ester compounds has not been markedly improved.

The formation of energetic ionic salts has been proven to be a simple and effective way to improve the energy and safety of compounds.[21–26] The cations, especially small cations like ammonium ions, which can functionalize as a bridge linking among molecules and layers to increase intra- and intermolecular forces by lots of hydrogen bonds. A typical example is dihydroxylammonium 5,5′-bis(tetrazolate-1*N*-oxide) (TKX-50). Yet, the synthesis of energetic salts based heterocyclic skeleton which incorporate nitrate ester group is rarely described and investigated.

In our previous work,[27] a few of energetic compounds and its ionic salts based on furazan–1,2,4-oxadiazole backbone with nitrate ester and nitramine moieties were synthesized, which exhibit low insensitivity and good detonation performance. Unfortunately, single crystal structures of these ionic salts have not been obtained. To have a better understanding of these structure–property relationships, two new kinds of energetic bicyclic frameworks, including furazan–isoxazole and furazan–1,3,4-oxadiazole, are constructed through [3+2] cycloaddition, and condensation cyclization, respectively. Corresponding furazan–isofurazan (isoxazole) based nitrate ester-methyl neutral compounds and their ammonium ions salts are obtained. An intensive research and comparison on the crystal structures, thermal decomposition processes and energetic properties of three kinds of furazan–isofurazan (isoxazole) ammonium ions salts are presented in this work.

Results and discussion

Synthetic procedures

Synthetic pathways of target compounds are shown in Scheme 2. Synthesis of **3d** and **3e** was previously described by our research group.[27] The starting material, compound **1a**, was prepared according to the literature.[28] The introduction of $-ONO_2$ into the skeleton requires using fuming nitric acid, H_2SO_4/HNO_3, 100% HNO_3 or other reagents as nitration reagents. When compound **1b** was treated with fuming nitric acid, only mixture products are obtained. To optimize the

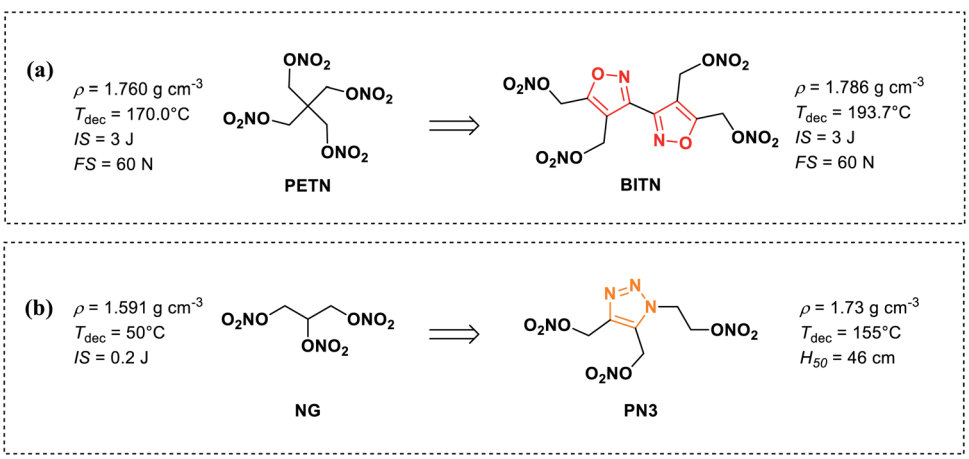

Scheme 1 The performance comparison between (a) PETN and BITN (b) NG and PN3.

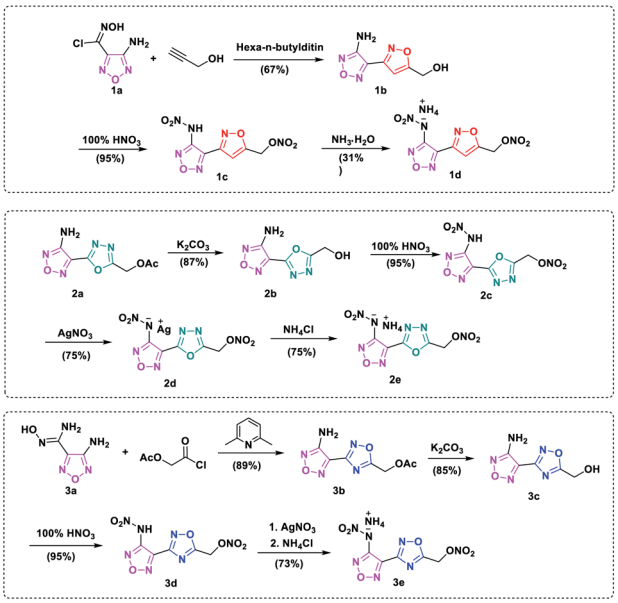

Scheme 2 Synthetic routes of energetic compound **1c**, **2c**, **3d** and their ionic salts **1d**, **2e**, **3e**. The synthetic routes of **3d** and **3e** have been report on our previous work ref. 25.

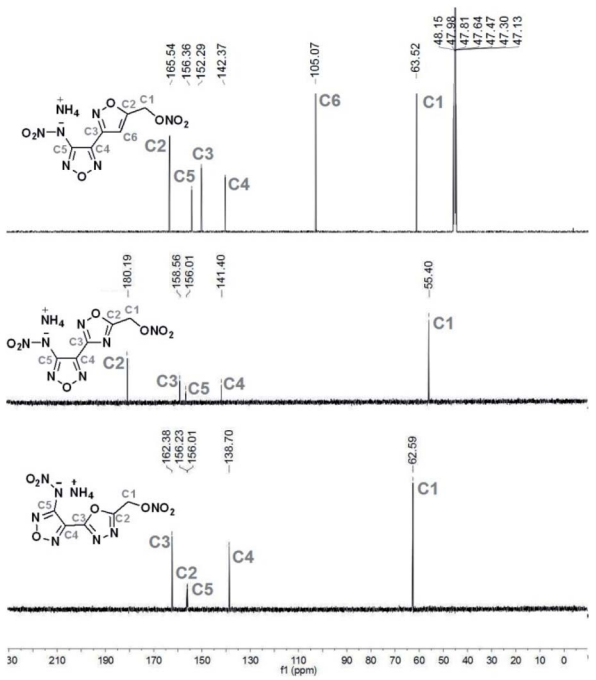

Fig. 2 The experimental ^{13}C NMR spectra of **1d** in CD_3OD, **2e** and **3e** in D_2O, respectively.

nitrating reaction, low temperature experiments were carried out in pure nitrate, and the required intermediate **1c** was obtained without purification and with high yield (95%). Compound **1c**, however, was unstable at room temperature in the absence of solvents. **1c** could be converted to its ammonium salt by adding aqueous ammonia in methanol solution. A suitable single crystal of compound **1d** was obtained by slow evaporation of the solvent at room temperature.

Compound **2a** was synthesized from dehydrate diaroylhydrazine in weakly alkaline solution. Then through reaction of off-protecting and nitration, compound **2c** could be obtained as light-yellow liquid, however, it was also found to be unstable at room temperature. The silver salt **2d** was firstly prepared in high yield by treating **2c** with $AgNO_3$ in methyl alcohol, then ammonium salt **2e** was synthesized by metathesis reaction in aqueous solution, as a colorless crystal solid.

All salts were characterized by IR, ^{1}H NMR and ^{13}C NMR spectroscopy. The ^{13}C NMR spectra of **1d**, **2e** and **3e** were shown in Fig. 2. The ^{13}C spectrum for **1d** was recorded in CD_3OD as solvent, while the spectra for **2e** and **3e** were determined in D_2O solution. All C-signals of each compound could be clearly observed. In contrast to **3e** (δ = 55.40 ppm), the signals for CH_2 group (C1) in **1d** (δ = 63.52 ppm) and **2e** (δ = 62.59 ppm) were shifted to higher field. For heterocyclic ring-connecting carbon atoms, the signals were observed in a typical range (105–180 ppm),[16,29–31] depending on the electron-withdrawing or pushing character of atoms attached.

X-ray crystallography

Suitable crystals for **1d** and **2e** were obtained by slow evaporation of their saturated solutions in a methanol/H_2O mixture, separately. The detailed crystal structure data (including selected bond lengths, angles, torsion angles and hydrogen bonds) were listed in Tables S1–S9.†

Salt **1d** crystallizes in the monoclinic space group $P2_1$, with two molecules per unit cell. The calculated density of 1.694 g cm^{-3} was determined from its X-ray crystal structure at 180(2) K. The atoms of diheterocycles and N–NO_2 in the anion were in nearly coplanar, supported by the dihedral angles of C1–N2–N1–O1 (−176.933 (445)°) and C2–C1–N2–N1 (−173.473 (461)°) (Fig. 3(a)). The bond lengths of C1–N2 [1.373(7) Å] and N1–N2 [1.317(6) Å] are shorter than normal carbon–carbon or carbon–nitrogen single bond length (*ca.* 1.54 Å) markedly,[32] suggesting that these atoms form a large π bond. However, the nitrate ester group and molecular skeleton formed a near right-angle (C4–C5–C6–O5 (105.398 (870)°)), and C6–O5 bond length [1.447(8) Å] was longer than that of a typical C–O bond (1.42 Å),[32] indicating that this bond was relatively weak.

Salt **2e** crystallizes in the monoclinic $P2_1/c$ space group with four formula units in the unit cell. **2e** displayed a calculated density of 1.758 g cm^{-3} at 150 K. The nitramino group and bicyclic scaffolds in **2e** were nearly coplanar and therefore form a conjugated system (Fig. 4(a)), as confirmed by the torsion angles of O4–C3–C4–C5 (170.362 (3)°) and C5–N6–N7–O6 (2.025 (6)°). The nitrate ester group and molecular skeleton formed an angle of nearly 90° (O4–C2–C1–O3 (72.788 (4)°) and N2–O2–C1–O3 (−111.138 (4)°), which were similar to the crystal structure of **1d**.

As show in Fig. 4(b) and (c), the supermolecular structure of **2e** was constructed by π–π stacking (the distance between the two neighbouring planes was 3.831 Å) and lots of hydrogen bonds among ammonium ions and atoms of energetic anions

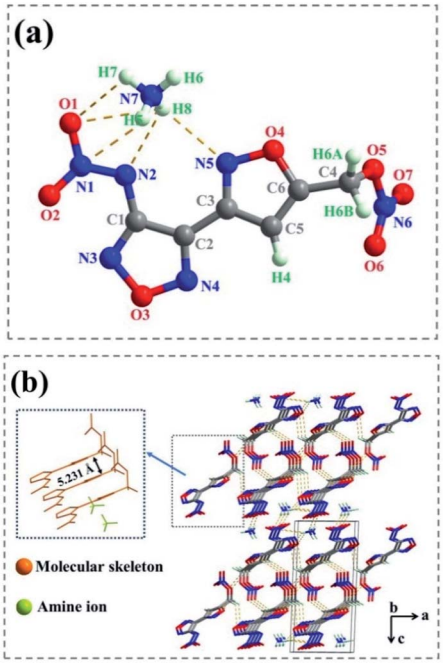

Fig. 3 (a) Thermal ellipsoid plot (50%) and labelling scheme for **1d**. (b) Packing diagram of **1d**.

were formed. There were nine kinds of intermolecular and intermolecular strong hydrogen bonds in the independent unit (Table S9†). While in **1d** (Fig. 3(b)), the ammonium ions were distributed on both sides of energetic anion layers and eleven kinds of strong hydrogen bonds were formed in the independent unit (Table S5†) (such as N7– H6···O3 [3.353 Å], N7–H6···N1 [3.051 Å], N7–H7···O4 [2.995 Å], N8–H6···N3 [2.281 Å] and so on).

To further investigating their weak inter-/intra molecular interaction, two-dimensional (2D)-fingerprint and relevant Hirshfeld surfaces of crystals **1d** and **2e** were fully studied. It was observed from the 2D fingerprint plot that O···H and N···H hydrogen bonds constitute 60% (**1d**) and 55% (**2e**) of the total weak interactions, respectively (Fig. 5(a) and (b)), which mainly concentrated in ammonium ions and nitro groups. This phenomenon demonstrates that introducing ammonium ions could greatly improve the ratios of intermolecular hydrogen bond interactions, and consequently to enhance the stability of molecules. In addition, compound **2e** has 5% percentage of N···N, N···C and C···N interactions which denoted π–π stacking. However, because of the "head to head" packing method of nitrate ester groups, both **1d** and **2e** had a percentage (12% and 14%) of O···O interactions which might lead to a decrease in decomposition temperatures. Overall, strong hydrogen-bond interactions and interlayer π–π stacking interactions could improve thermal stability of energetic salts, which is consistent with the experimental decomposition temperature.

ESP analysis and thermal behaviours

Thermal behaviors of **1d**, **2e** and **3e** were investigated and compared by DSC under a heating rate of 10 °C min^{-1} in Ar atmosphere. Due to the presence of nitramino groups, molecule energetic compounds **1c** and **2c** were unstable at room temperature. Compared with the corresponding molecular compounds, the decomposition temperatures of the salts **1d**, **2e** and **3e** increased by more than 110 °C (Fig. 7). Among them, **1d** exhibits relatively good thermal stability (144.76 °C), which is

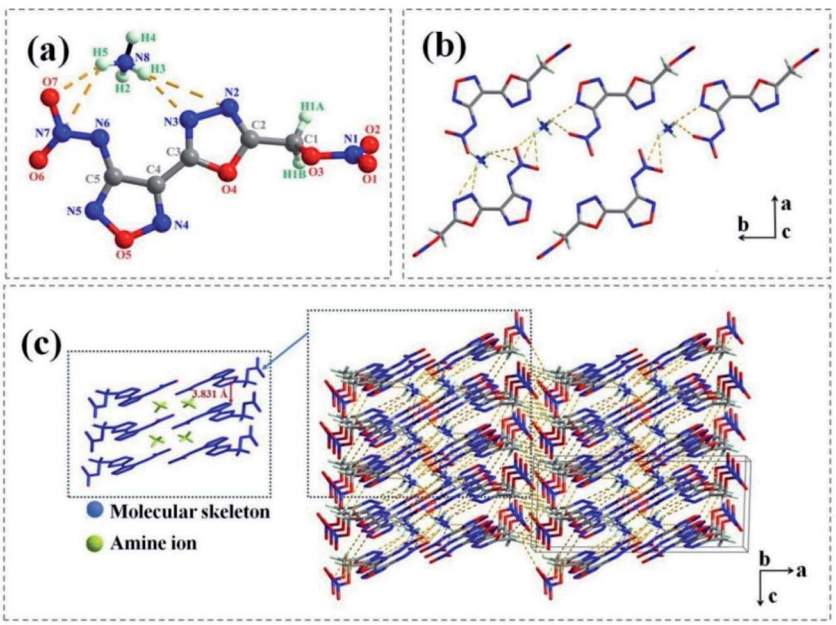

Fig. 4 (a) Thermal ellipsoid plot (50%) and labelling scheme for **2e**. (b) The 2D layer formed of **2e**. Dashed lines indicate strong hydrogen bonding. (c) Packing diagram of **2e**.

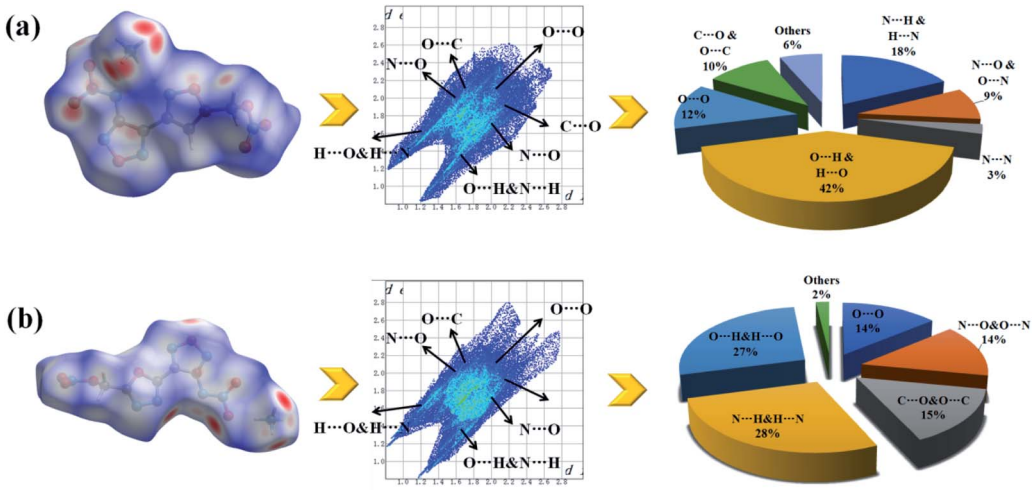

Fig. 5 Hirshfeld surfaces calculation (white, distance *d* equals the van der Waals distance; blue, *d* exceeds the van der Waals distance; red, *d* is less than van der Waals distance) and two-dimensional fingerprint plots of (a) **1d** and (b) **2e**.

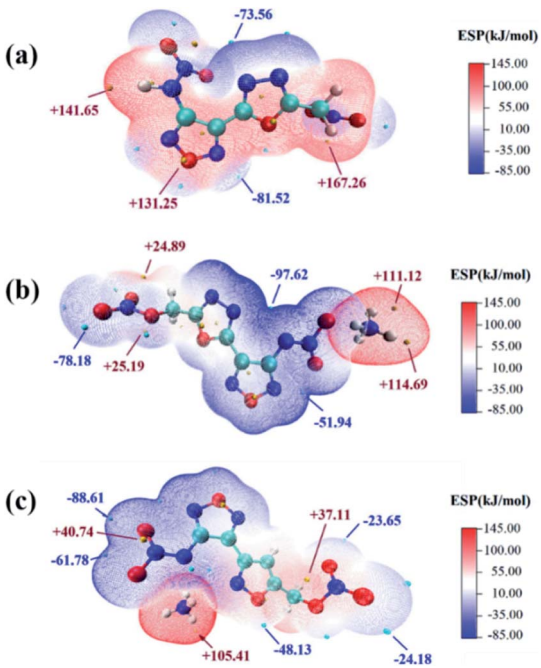

Fig. 6 Electrostatic potential surfaces of compounds (a) **2d**, (b) **2e** and (c) **1d**. The minimum and maximum of ESP are marked as blue and red points, respectively. The maximum value of ESP is labeled with red texts and units are in kcal mol^{-1}.

consistent with the two-dimensional (2D)-fingerprint analysis result.

To understand the influence of the energetic groups on the charge distribution of molecules, electrostatic potential energy surface (ESP) analysis of **1d**, **2d** and **2e** was performed by using Multiwfn.[33,34] The optimized structure of **2e** was carried out based upon the B3LYP/6-31+G**[35] method by Gaussian 09 software.[36] As shown in Fig. 6, in contrast to compound **2d**, salts **1d** and **2e** exhibited lower ESP maximum values and more negative charge accumulation in heterocyclic backbone, which might lead to relatively higher thermal stability.

The thermal decomposition processes of **1d**, **2e** and **3e** were further investigated using non-isothermal kinetic study and compared by Kissinger's method.[37] In general, the kinetic parameters included the apparent activation energy (E_k), the per-exponential factor (A) and the linear coefficient (r) of the first exothermic decomposition process. The DSC traces of compounds were obtained at various heating rates (2.5, 5, 10 and 15 °C). As shown in Fig. 7, the linear fitting of **1d**, **2e** and **3e** was straight lines with $r = 0.997$, 0.996 and 0.992, respectively, and it was demonstrated that Kissinger method is applied to calculate the thermal kinetic parameters. The apparent activation energy (E_k) of **1d**, **2e** and **3e** were about 148.57 kJ mol^{-1}, 186.91 kJ mol^{-1} and 148.98 kJ mol^{-1}, respectively (Table S10†), and it was indicated that **2e** displayed best stability at thermodecomposition process.

Computational energetic properties

The enthalpy of formation was one of the significant energetic characteristics of energetic compound. The heats of formation in solid phase (ΔH_f) for **1d** and **2e** were calculated using the heat of formation in gas phase and heat of phase transition (lattice energy) according to the Born–Haber energy cycle.[38] The gas-state enthalpies and energies of formation of molecule, cations, and anions were calculated using the quantum chemical CBS-4M calculations (H_{CBS-4M}) method.[39,40] **1d**, **2e** and **3e** had positive heats of formation of 265.1, 253.5 and 243.3 kJ mol^{-1}, respectively (Table 1), which exceeded those of PETN (−538.6 kJ mol^{-1}) and RDX (92.6 kJ mol^{-1}).

The detonation performances of these salts were calculated using the EXPLO5 program (version 6.01)[41] based on the calculated heats of formation and densities. The calculated detonation velocity (D) and pressure (P) values were shown in Table 1. Among these three kinds of salts based on bicyclic scaffolds of furazan–isofurazan (isoxazole), 1,2,4-oxadiazole-

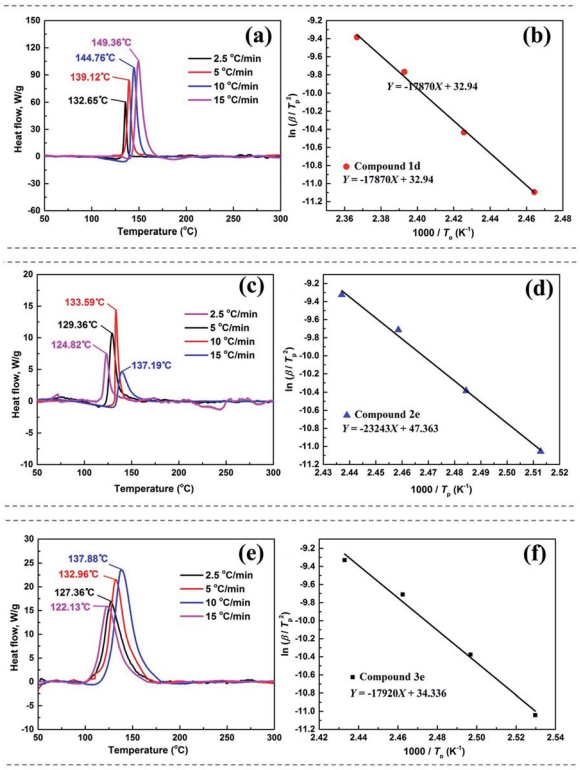

Fig. 7 DSC traces of (a) **1d**, (c) **2e** and (e) **3e** obtained at various heating rates. Kissinger's plots of (b) **1d**, (d) **2e** and (f) **3e**.

furazan based salt **3e** displayed the best detonation performance (D: 8428 m s^{-1}; P: 35 GPa), which is slightly better than PETN (D: 8400 m s^{-1}; P: 32 GPa).

The impact sensitives of the salts **1d** and **2e** were determined by following BAM standard methods. Both salts showed excellent mechanical performance (IS > 30 J) due to strong non-covalent interactions, which was greatly superior to RDX and most reported nitrate ester energetic compounds, such as NG (IS < 0.2 J), PETN (IS = 3 J) and BOM (IS = 8.7 J).

Conclusions

In summary, two new heterocyclic based neutral compound nitrate ester compounds (**1c** and **2d**) and its ammonium salts (**1d** and **2e**) were synthesized and fully investigated. However, both neutral nitrate ester compounds were unstable at room temperature. By introducing ammonium ion, the decomposition temperatures of **1d**, **2e** and **3e** were greatly improved over 110 °C. Among them, **1d** exhibits relatively good thermal stability (144.8 °C) probably due to more strong hydrogen bond interactions besides π–π stacking in its crystal structure. Among these three kinds of salts based on bicyclic scaffolds of furazan–isofurazan (isoxazole), 1,2,4-oxadiazole-furazan based salt **3e** exhibits good detonation performance and excellent mechanical performance, higher than most reported nitrate ester energetic compounds. The result indicated that introducing positive ion is a good strategy to decreasing mechanical sensitivity and thermal stability of nitrate ester compounds.

Experimental

Reagents and sample preparation

Tris(hydroxymethyl)nitromethane was supplied by Xi'an Modern Chemistry Research Institute. All reagents and solvents were purchased from Aladdin Bio-Chem Technology CO., Ltd (Shanghai, China) and used without further purification unless otherwise indicated.

Apparatus and measurements

^{13}C and ^{1}H NMR spectra were measured with AV 500 NMR spectrometer (Bruker, Switzerland). Infrared spectra were measured by an EQUINOX 55 Fourier transform Infrared spectrometer (Bruker, Germany). Elemental analyses were performed with the vario EL cube elemental analyzer (Elementar, Germany).

The thermal analysis experiments were performed with a model TGA/DSC 1 instrument (METTLER, Switzerland). Single crystal X-ray experiment was carried out on a Bruker Apex II CCD diffractometer equipped with graphite monochromatized Ga and Cu Kα radiation using ω and φ scan mode. Structures were solved by the direct method using SHELXTL and refined by means of full-matrix least-squares procedures on F^2 with the programs SHELXL-97. All nonhydrogen atoms were refined with anisotropic displacement parameters. The sensitivity towards impact (IS) was determined according to BAM standards.

Table 1 Physiochemical properties and detonation performances of compounds **1d**, **2e** and **3e**

Compound	T_d[a]/°C	ρ/g cm^{-1}	OB[c]/%	ΔH_f[d]/kJ mol^{-1}	D[f]/m s^{-1}	P[e]/Gpa	IS/J
1d	144.8	1.674[b]	−47	265.1	7980	27	35[g]
2e	132.4	1.758[b]	−33	243.3	8361	31	33[g]
3e[19]	135	1.79	−33	253.5	8428	35	32
RDX	204	1.80	−21	92.6	8795	35	7.5
PETN[9]	172.9	1.76	−10	−538.6	8400	32	3
BOM[19]	183.4	1.832	−33	−79.4	8180	29.4	8.7

[a] Decomposition temperature (°C). [b] Densities obtained from X-ray measurements. [c] Oxygen balance (OB, %) for a compound with a molecular formula of CaHbNcOd without crystal water. [d] Standard enthalpy of formation (at 298 K, kJ mol^{-1}). [e] Detonation pressure (GPa). [f] Detonation velocity (m s^{-1}). [g] Impact sensitivity (J).

DFT calculations

All quantum chemical calculations were carried out using the program package Gaussian 09. The geometry optimizations of the molecules and frequency analyses were accomplished by using the B3LYP with the 6-311+G** basis set. The ESP analysis of **1c** was carried out based upon the B3LYP/6-31+G** method by Gaussian 09 software with optimized structure. The ESP analyses of **1d** and **2e** were carried out based on corresponding single crystal structures. The gas-state enthalpies and energies of formation of molecules were calculated using the quantum chemical CBS-4M calculations ($H_{CBS\text{-}4M}$) method in order to obtain accurate values.

Synthesis

3-(4-Aminofurazan-3-ly)-5-hydroxymethylisoxazole (1b). The starting material 4-aminofurazan-3-carbohydroximoyl chloride (**1a**, 0.4 g, 2.46 mmol) was dissolved in diethyl ether (20 mL), then proparagyl alcohol (0.7 g, 0.012 mol) and hexa-*n*-butylditin (1.4 g, 2.46 mmol) were added at room temperature. The reaction mixture was stirred in lighting conditions for 12 h. The organic solvent was evaporated to give crude compound, then washed with ethyl alcohol (10 mL × 3), the product **1b** was obtained as colorless solid (0.35 g, 67%). mp143 °C, DSC (10 °C min^{-1}, onset) 310.79 °C (decomp.).^{1}H NMR (DMSO-d_6, 500 MHz) δ: 6.427 (s, 2H, NH_2), 5.687–5.663 (t, J = 6.0 Hz, 1H, OH), 5.131–5.110 (t, J = 5.0 Hz, 1H, OH), 4.737–4.725 (d, J = 6.0 Hz, 2H, CH_2); 4.633–4.623 (d, J = 5.0 Hz, 2H, CH_2); ^{13}C NMR (DMSO-d_6, 500 MHz) δ: 170.644, 155.349, 151.150, 138.518, 115.689, 53.217, 51.862; IR (KBr) υ (cm^{-1}): 3472, 3349, 3291, 2956–2869, 1635,1552; anal. calcd for $C_7H_8N_4O_4$: C 39.62, H 3.774, N 26.41; found C 39.74, H 3.752, N 25.64.

Ammonium 3-(4-nitraminofurazan-3-ly)-isoxazole-5-methylnitrate (1d). Compound **1b** (0.4 g, 2.20 mmol) was carefully added to the 100% HNO_3 (7 mL) while maintaining the temperature at 0–5 °C. After complete addition, the solution was stirred for 1 h. The mixture was poured into ice cold water (60 mg), followed by extraction with ethyl acetate (20 mL × 2). The organic phase was washed by saturated salt water (10 mL × 3), dried with $MgSO_4$. After filtrating the precipitate, conc. ammonia (0.2 mL) was then added dropwise in the solvation and the mixture was stirred at room temperature for 12 h, **1d** obtained as faint yellow solid (0.21 g, 0.73 mmol). DSC (10 °C min^{-1}, T_p) 144.8 °C (decomp.). ^{13}C NMR (CD_3OD-d_6, 125 MHz): δ = 165.56, 156.38, 152.30, 142.39, 105.07, 63.52; ^{1}H NMR (CD_3OD-d_6, 500 MHz): δ = 7.17 (s, 1H), 5.79 (s, 2H); IR (KBr, cm^{-1}): 3156, 3028, 2911, 1651, 1643, 1619, 1513, 1433, 1400, 1341, 1309, 1281, 1187, 1091, 1018, 947, 911, 871, 850, 821, 778, 759; anal. calcd for $C_6H_7N_7O_7$: C 24.92, H 2.44, N 33.91; found C 24.74, H 2.74, N 33.01.

5-(4-Amino-furazan-3-ly)-1,3,4-oxadiazole-2-methylene acetate (2b). Compound **2a** (2.00 g, 8.88 mmol) was added to a mixture of K_2CO_3 (1.47 g, 10.66 mmol), H_2O (2 mL) and methanol (30 mL) at room temperature. The mixture was stirred at room temperature for 24 h. The reaction mixture was concentrated *in vacuo* to give a crude solid. The pure production was obtained and purified with 20 mL H_2O and collected as a white solid (1.42 g, 7.73 mmol). ^{13}C NMR (DMSO-d_6, 125 MHz): δ = 167.59, 155.68, 155.52, 135.43, 54.07; ^{1}H NMR (500 MHz, DMSO-d_6) δ = 6.64 (s, 2H), 6.09 (t, J = 6.4 Hz, 1H), 4.79 (d, J = 6.3 Hz, 2H). Anal. calcd for $C_7H_7N_5O_4$: C 37.34, H, 3.13, N 31.10; found C 37.65, H 3.24, N 30.01.

5-(4-Nitraminofurazan-3-ly)-1,3,4-oxadiazole-2-methylnitrate (2c). Compound **2b** (0.4 g, 2.18 mmol) was carefully added to the 100% HNO_3 (7 mL) while maintaining the temperature at 0–5 °C. After complete addition, the solution was stirred for 1 h. The mixture was poured into ice cold water (60 mg) followed by extraction with ethyl acetate (20 mL × 2). The organic phase was washed by saturated salt water (10 mL × 3), dried with $MgSO_4$. The solvent was evaporated under reduced pressure to yield **2c** as light-yellow liquid which is unstable at room temperature.

Ammonium 5-(4-nitraminofurazan-3-ly)-1,3,4-oxadiazole-2-methylnitrate (2e). Compound **2c** was diluted with 10 mL methanol, and the solution of silver nitrate was carefully added. The mixture was stirred for 2 h. After filtrating, the silver salt of **2c** was obtained as a faint yellow solid. The ammonium chloride (3 mmol) was dissolved in water (5 mL), the silver salt of **2c** was added. After stirring for 2 h at room temperature, the precipitation was filtered. The solution was evaporated to dryness to obtain **2e** as a faint yellow solid. DSC (10 °C min^{-1}, T_p) 132.4 °C (decomp.). ^{1}H NMR (500 MHz, deuterium oxide) δ 5.99 (s, 2H). ^{13}C NMR (126 MHz, deuterium oxide) δ 162.36, 156.22, 155.99, 138.68, 62.59. Anal. calcd for $C_5H_6N_8O_7$: C 20.70, H 2.08, N 38.60; found C 20.53, H 2.31, N 39.04.

Conflicts of interest

There are no conflicts to declare.

Acknowledgements

We are grateful to the financial support from National Natural Science Foundation of China (No. 22175139).

Notes and references

1 M. Smiljkovic, M. T. Matsoukas, E. Kritsi, U. Zelenko, S. G. Grdadolnik, R. C. Calhelha, I. C. F. R. Ferreira, S. Sankovic-Babic, J. Glamoclija, T. Fotopoulou, M. Koufaki, P. Zoumpoulakis and M. Sokovic, *ChemMedChem*, 2018, **13**, 251–258.
2 S. Warren and G. Francis, *Am. J. Med.*, 1978, **65**, 53–62.
3 P. R. Sage, I. S. de la Lande, I. Stafford, C. L. Bennett, G. Phillipov, J. Stubberfield and J. D. Horowitz, *Circulation*, 2000, **102**, 2810–2815.
4 J. T. Flaherty, P. Reid, D. Kelly, D. Taylor, M. Weisfeldt and B. Pitt, *Circulation*, 1975, **51**, 132–139.
5 C. P. Zhang, X. M. Zhai, Y. J. Li and Z. G. Sun, *Adv. Mater. Res.*, 2012, **354**, 462–467.
6 E. R. Jonash, J. D. Wear and W. P. Cook, *Effect of Fuel Additives on Carbon Deposition in a J33 Single Combustor: Nine Oxygen-bearing Compounds*, National Advisory Committee for Aeronautics, 1956.

7 D. E. Chavez, M. A. Hiskey, D. L. Naud and D. Parrish, *Angew. Chem.*, 2008, **120**, 8431–8433.
8 Z.-D. Sun, X. L. Fu, H. J. Yu, X. Z. Fan and X. H. Ju, *J. Hazard. Mater.*, 2017, **339**, 401–408.
9 J. J. Sabatini and E. C. Johnson, *ACS Omega*, 2021, **6**, 11813–11821.
10 T. M. Klapötke, B. Krumm, T. Reith and C. Riedelsheimer, *ChemistrySelect*, 2021, **6**, 8581–8586.
11 J. Dong, Q. L. Yan, P. J. Liu, W. He, X. F. Qi and S. Zeman, *J. Therm. Anal. Calorim.*, 2018, **131**, 1391–1403.
12 A. T. Camp, H. S. Haiss and P. R. Mosher, *Energetic Plasticizer and Improved Gas Producing Charges*, Department of The Navy, Washington DC, 1993.
13 A. Booth and F. Llewellyn, *J. Chem. Soc.*, 1947, 837–846.
14 K. A. S. Stark, J. F. Alvino, K. P. Kirkbride, C. J. Sumby, G. F. Metha, C. E. Lenehan, M. Fitzgerald, C. Wall, M. Mitchell and C. Prior, *Propellants, Explos., Pyrotech.*, 2019, **44**, 541–549.
15 Y. Li, Y. Shu, B. Wang, S. Zhang and L. Zhai, *RSC Adv.*, 2016, **6**, 84760–84768.
16 L. A. Wingard, E. C. Johnson, P. E. Guzmán, J. J. Sabatini, G. W. Drake, E. F. C. Byrd and R. C. Sausa, *Eur. J. Org. Chem.*, 2017, **2017**, 1765–1768.
17 J. Zhang, P. Yin, L. A. Mitchell, D. A. Parrish and J. n. M. Shreeve, *J. Mater. Chem. A*, 2016, **4**, 7430–7436.
18 L. Bauer, M. Benz, T. M. Klapötke, T. Lenz and J. Stierstorfer, *J. Org. Chem.*, 2021, **86**, 6371–6380.
19 E. C. Johnson, J. J. Sabatini, D. E. Chavez, R. C. Sausa, E. F. C. Byrd, L. A. Wingard and P. E. Guzmàn, *Org. Process Res. Dev.*, 2018, **22**, 736–740.
20 P. Gaur, S. Dev, S. Kumar, M. Kumar, A. A. Vargeese, P. Soni, P. F. Siril and S. Ghosh, *ACS Omega*, 2017, **2**, 8227–8233.
21 Q. Wang, Y. Shao and M. Lu, *Cryst. Growth Des.*, 2019, **20**, 197–205.
22 Y. Xu, L. Tian, D. Li, P. Wang and M. Lu, *J. Mater. Chem. A*, 2019, **7**, 12468–12479.
23 J. Ren, W. Zhang, T. Zhang, Y. Yin, L. Wang, Z. Li, Q. Zeng and T. Zhang, *J. Energ. Mater.*, 2021, **39**, 48–59.
24 C. He, G. H. Imler, D. A. Parrish and J. n. M. Shreeve, *J. Mater. Chem. A*, 2018, **6**, 16833–16837.
25 C. Lei, H. Yang and G. Cheng, *Dalton Trans.*, 2020, **49**, 1660–1667.
26 P. Yang, H. Yang, Y. Zhao, J. Tang and G. Cheng, *Dalton Trans.*, 2021, **50**, 16499–16503.
27 Q. Xue, F. q. Bi, J. l. Zhang, Z. j. Wang, L. j. Zhai, H. Huo, B. z. Wang and S. y. Zhang, *Front. Chem.*, 2020, **7**, 942.
28 J. Zhang, L. A. Mitchell, D. A. Parrish and J. n. M. Shreeve, *J. Am. Chem. Soc.*, 2015, **137**, 10532–10535.
29 L. L. Fershtat, A. S. Kulikov, I. V. Ananyev, M. I. Struchkova and N. N. Makhova, *J. Heterocycl. Chem.*, 2016, **53**, 102–108.
30 S. D. Shaposhnikov, N. V. Korobov, A. V. Sergievskii, S. V. Pirogov, S. F. Mel'nikova and I. V. Tselinskii, *Russ. J. Org. Chem.*, 2002, **38**, 1351–1355.
31 Z. Fu, R. Su, Y. Wang, Y. F. Wang, W. Zeng, N. Xiao, Y. Wu, Z. Zhou, J. Chen and F. X. Chen, *Chem.–Eur. J.*, 2012, **18**, 1886–1889.
32 F. H. Allen, O. Kennard, D. G. Watson, L. Brammer, A. G. Orpen and R. Taylor, *J. Chem. Soc., Perkin Trans. 2*, 1987, S1–S19.
33 T. Lu and F. Chen, *J. Comput. Chem.*, 2012, **33**, 580–592.
34 S. Manzetti and T. Lu, *J. Phys. Org. Chem.*, 2013, **26**, 473–483.
35 J. L. Calais, *Int. J. Quantum Chem.*, 1993, **47**, 101.
36 M. Frisch, G. Trucks, H. B. Schlegel, G. Scuseria, M. Robb, J. Cheeseman, G. Scalmani, V. Barone, B. Mennucci and G. Petersson, *Gaussian 09*, Gaussian Inc., Wallingford, CT, 2009, vol. 200, p. 28.
37 R. L. Blaine and H. E. Kissinger, *Thermochim. Acta*, 2012, **540**, 1–6.
38 H. D. B. Jenkins, D. Tudela and L. Glasser, *Inorg. Chem.*, 2002, **41**, 2364–2367.
39 J. W. Ochterski, G. A. Petersson and J. A. Montgomery Jr, *J. Chem. Phys.*, 1996, **104**, 2598–2619.
40 J. A. Montgomery Jr, M. J. Frisch, J. W. Ochterski and G. A. Petersson, *J. Chem. Phys.*, 2000, **112**, 6532–6542.
41 M. Suceska, *EXPLO5, version*, Brodarski Institute, Zagreb, Croatia, 2013.